Sensing atmospheric reactive species using light emitting diode by incoherent broadband cavity enhanced absorption spectroscopy

Hongming Yi,[1,4] Tao Wu,[2] Guishi Wang,[3] Weixiong Zhao,[3] Eric Fertein,[1] Cécile Coeur,[1] Xiaoming Gao,[3] Weijun Zhang,[3] and Weidong Chen[1,*]

[1]*Laboratory of Physical Chemistry of the Atmosphere, University of the Littoral Opal Coast, Dunkirk, France*
[2]*Nanchang Hangkong University, Nanchang, China*
[3]*Anhui Institute of Optics and Fine Mechanics, Chinese Academy of Sciences, Hefei, China*
[4]*now with National Institute of Standards and Technology, Gaithersburg, Maryland, USA*
**chen@univ-littoral.fr*

Abstract: We overview our recent progress in the developments and applications of light emitting diode-based incoherent broadband cavity enhanced absorption spectroscopy (LED-IBBCEAS) techniques for real-time optical sensing chemically reactive atmospheric species (HONO, NO_3, NO_2) in intensive campaigns and in atmospheric simulation chamber. New application of optical monitoring of NO_3 concentration-time profile for study of the NO_3-initiated oxidation process of isoprene in a smog chamber is reported.

OCIS codes: (280.4788) Optical sensing and sensors; (120.6200) Spectrometers and spectroscopic instrumentation; (010.1120) Air pollution monitoring.

References and links

1. W. Chen, R. Maamary, X. Cui, T. Wu, E. Fertein, D. Dewaele, F. Cazier, Q. Zha, Z. Xu, T. Wang, Y. Wang, W. Zhang, X. Gao, W. Liu, and F. Dong, "Photonic Sensing of Environmental Gaseous Nitrous Acid (HONO): Opportunities and Challenges," in *The Wonder of Nanotechnology: Quantum Optoelectronic Devices and Applications*, M. Razeghi. L. Esaki, and K. von Klitzing, Eds., SPIE Press, Bellingham, WA, pp. 693–737 (2013).
2. H. Yi, R. Maamary, X. Gao, M. W. Sigrist, E. Fertein, and W. Chen, "Short-lived species detection of nitrous acid by external-cavity quantum cascade laser based quartz-enhanced photoacoustic absorption spectroscopy," Appl. Phys. Lett. **106**(10), 101109 (2015).
3. D. S. Venables, T. Gherman, J. Orphal, J. C. Wenger, and A. A. Ruth, "High sensitivity in situ monitoring of NO_3 in an atmospheric simulation chamber using incoherent broadband cavity-enhanced absorption spectroscopy," Environ. Sci. Technol. **40**(21), 6758–6763 (2006).
4. R. M. Varma, D. S. Venables, A. A. Ruth, U. Heitmann, E. Schlosser, and S. Dixneuf, "Long optical cavities for open-path monitoring of atmospheric trace gases and aerosol extinction," Appl. Opt. **48**(4), B159–B171 (2009).
5. S. E. Fiedler, A. Hese, and A. A. Ruth, "Incoherent broad-band cavity-enhanced absorption spectroscopy," Chem. Phys. Lett. **371**(3-4), 284–294 (2003).
6. S. M. Ball, J. M. Langridge, and R. L. Jones, "Broadband cavity enhanced absorption spectroscopy using light emitting diodes," Chem. Phys. Lett. **398**(1-3), 68–74 (2004).
7. J. M. Langridge, S. M. Ball, A. J. L. Shillings, and R. L. Jones, "A broadband absorption spectrometer using light emitting diodes for ultrasensitive, in situ trace gas detection," Rev. Sci. Instrum. **79**(12), 123110 (2008).
8. R. A. Washenfelder, A. R. Attwooda, J. M. Flores, Y. Rudich, and S. S. Brown, "Broadband cavity enhanced spectroscopy in the ultraviolet spectral region for measurements of nitrogen dioxide and formaldehyde," Atmos. Meas. Tech. **9**(1), 41–52 (2016).
9. K.-E. Min, R. A. Washenfelder, W. P. Dubé, A. O. Langford, P. M. Edwards, K. J. Zarzana, J. Stutz, K. Lu, F. Rohrer, Y. Zhang, and S. S. Brown, "A broadband cavity enhanced absorption spectrometer for aircraft measurements of glyoxal, methylglyoxal, nitrous acid, nitrogen dioxide, and water vapor," Atmos. Meas. Tech. **9**(2), 423–440 (2016).
10. D. Romanini, I. Ventrillard, G. Méjean, J. Morville, and E. Kerstel, "Introduction to cavity enhanced absorption spectroscopy," in Springer Series in Optical Sciences (2014), pp. 1–60.
11. W. Chen, A. A. Kosterev, F. K. Tittel, X. Gao, and W. Zhao, "H_2S trace concentration measurements using Off-Axis Integrated Cavity Output Spectroscopy in the near-infrared," Appl. Phys. B **90**(2), 311–315 (2008).
12. A. A. Ruth, S. Dixneuf, and R. Raghunandan, "Broadband cavity-enhanced absorption spectroscopy with

#257569 Received 19 Jan 2016; revised 17 Feb 2016; accepted 19 Feb 2016; published 24 Mar 2016

incoherent light," in Springer Series in Optical Sciences (2014), pp. 485–517.
13. http://satellite.mpic.de/spectral_atlas.
14. W. Zhao, X. Xu, M. Dong, W. Chen, X. Gu, C. Hu, Y. Huang, X. Gao, W. Huang, and W. Zhang, "Development of a cavity-enhanced aerosol albedometer," Atmos. Meas. Tech. **7**(8), 2551–2566 (2014).
15. J. Chen and D. S. Venables, "A broadband optical cavity spectrometer for measuring weak near-ultraviolet absorption spectra of gases," Atmos. Meas. Tech. **4**(3), 425–436 (2011).
16. M. Dong, W. Zhao, M. Huang, W. Chen, C. Hu, X. Gu, S. Pei, W. Huang, and W. Zhang, "Near-ultraviolet incoherent broadband cavity enhanced absorption spectroscopy for OClO and CH_2O in Cl-initiated photooxidation experiment," Chin. J. Chem. Phys. **26**(2), 133–139 (2013).
17. A. L. Gomez and E. P. Rosen, "Fast response cavity enhanced ozone monitor," Atmos. Meas. Tech. **6**(2), 487–494 (2013).
18. S. Vaughan, T. Gherman, A. A. Ruth, and J. Orphal, "Incoherent broad-band cavity-enhanced absorption spectroscopy of the marine boundary layer species I_2, IO and OIO," Phys. Chem. Chem. Phys. **10**(30), 4471–4477 (2008).
19. T. Wu, W. Chen, E. Fertein, F. Cazier, D. Dewaele, and X. Gao, "Development of an open-path incoherent broadband cavity-enhanced spectroscopy based instrument for simultaneous measurement of HONO and NO_2 in ambient air," Appl. Phys. B **106**(2), 501–509 (2012).
20. T. Wu, Q. Zha, W. Chen, Z. Xu, T. Wang, and X. He, "Development and deployment of a cavity enhanced UV-LED spectrometer for measurements of atmospheric HONO and NO_2 in Hong Kong," Atmos. Environ. **95**, 544–551 (2014).
21. T. Wu, C. Coeur-Tourneur, G. Dhont, A. Cassez, E. Fertein, X. He, and W. Chen, "Simultaneous monitoring of temporal profiles of NO_3, NO_2 and O_3 by incoherent broadband cavity enhanced absorption spectroscopy for atmospheric applications," J. Quant. Spectrosc. Radiat. Transf. **133**, 199–205 (2014).
22. R. G. Prinn, "The cleansing capacity of the atmosphere," Annu. Rev. Environ. Resour. **28**(1), 29–57 (2003).
23. B. J. Finlayson-Pitts and J. N. Pitts, Jr., *Chemistry of the Upper and Lower Atmosphere* (Academic Press, 2000).
24. A. Saiz-Lopez, J. A. Shillito, H. Coe, and J. M. C. Plane, "Measurements and modelling of I_2, IO, OIO, BrO and NO_3 in the mid-latitude marine boundary layer," Atmos. Chem. Phys. **6**(6), 1513–1528 (2006).
25. G. Berthet, J.-B. Renard, M. Chartier, M. Pirre, and C. Robert, "Analysis of OBrO, IO, and OIO absorption signature in UV-visible spectra measured at night and at sunrise by stratospheric balloon-borne instruments," J. Geophys. Res. **108**(D5), 14649–14663 (2003).
26. O. J. Kennedy, B. Ouyang, J. M. Langridge, M. J. S. Daniels, S. Bauguitte, R. Freshwater, M. W. McLeod, C. Ironmonger, J. Sendall, O. Norris, R. Nightingale, S. M. Ball, and R. L. Jones, "An aircraft based three channel broadband cavity enhanced absorption spectrometer for simultaneous measurements of NO_3, N_2O_5 and NO_2," Atmos. Meas. Tech. **4**(9), 1759–1776 (2011).
27. IPCC Scientific Assessment Climate Change, J. T. Houghton ed. (Cambridge University Press, 1992).
28. FACSIMILE, MCPA, *http://www.mcpa-software.com/facsimileframe.html.*
29. R. Atkinson, D. L. Baulch, R. A. Cox, J. N. Crowley, R. F. Hampson, R. G. Hynes, M. E. Jenkin, M. J. Rossi, and J. Troe; IUPAC Subcommittee, "Evaluated kinetic and photochemical data for atmospheric chemistry: Volume II – gas phase reactions of organic species," Atmos. Chem. Phys. **6**(11), 3625–4055 (2006).
30. R. Atkinson, "Kinetics and mechanisms of the gas-phase reactions of the NO_3 radical with organic compounds," J. Phys. Chem. Ref. Data **20**(3), 459–507 (1991).

1. Introduction

Reliable concentration assessment of the major atmospheric oxidants (hydroxyl free radicals, nitrate radicals, and ozone, etc), and their precursors (nitrous acid, nitrogen dioxide, and formaldehyde) is essential for understanding and predicting chemical processes that affect regional air quality and global climate change. Real-time in situ monitoring of these chemically short-lived atmospheric constituents is challenging because of their high reactivity, short lifetimes on the order of minutes or less [1,2] and ultralow concentrations from ppbv (parts per billion by volume) to sub-pptv (parts per trillion by volume) [1–4]. Incoherent broadband cavity enhanced absorption spectroscopy (IBBCEAS), introduced by Fiedler et al. in 2003 [5] combining broadband light source with high-finesse optical cavity, offers the unique capacity of high-sensitivity measurement of multiple species. Based on a ~1 m long optical cavity, effective absorption path length of up to 1-10 km can be achieved, which allows for significant enhancement of detection sensitivity while keeping the setup very compact and suitable for high spatial-resolution measurements. The use of broadband light sources (such as Xenon arc lamp [3,5], light emitting diodes (LEDs) [6,7], or supercontinuum sources [8]) as probing spectral light allows for simultaneous quantitative assessment of multiple atmospheric species [3–9]. In addition, IBBCEAS method eliminates the need for optical mode matching and electronic locking of the cavity resonant mode to the

#257569 Received 19 Jan 2016; revised 17 Feb 2016; accepted 19 Feb 2016; published 24 Mar 2016

laser wavelength, as required for cavity ring-down spectroscopy (CRDS) [10]. IBBCEAS does not require particular optical alignment as used in off-axis integrated cavity output spectroscopy (OA-ICOS) [11], which makes IBBCEAS apparatus much simple, more stable and robust.

LEDs, widely used today in lighting and video displays and available for the spectral region from the ultraviolet (UV) to the visible, allow access to the spectral regions that involve strong fundamental electronic transitions of gaseous molecules (Fig. 1). LED is a very suitable and truly cost effective light source, resulting from its mass production, for IBBCEAS applications [12].

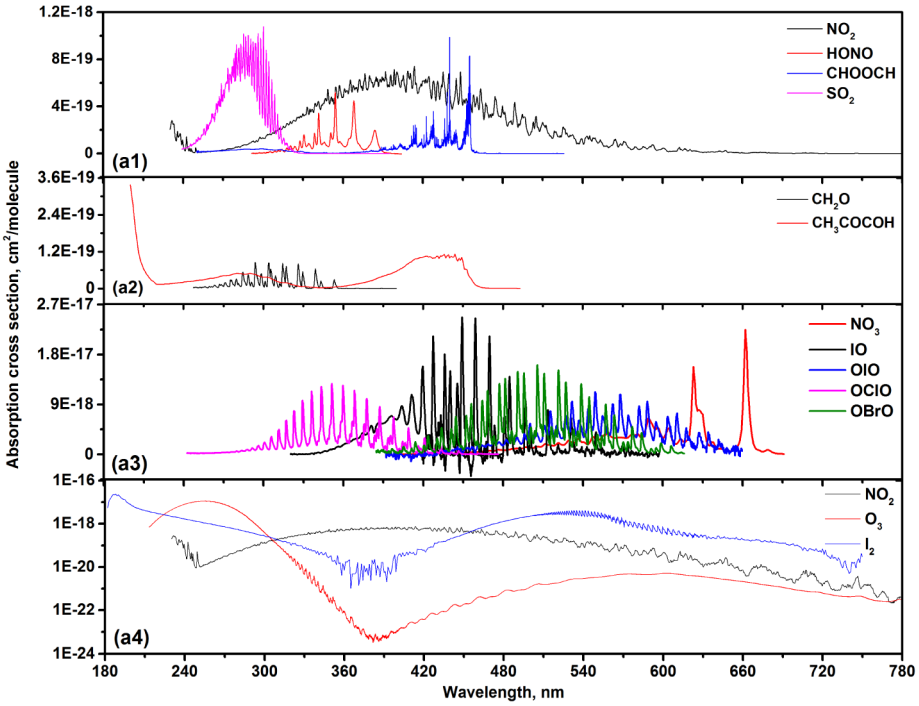

Fig. 1. Spectra of key atmospheric molecular species in the ultraviolet and visible region [13]

Over the last decade, LED-based IBBCEAS technique has been increasingly developed for sensitive measurements of aerosol extinction [4,14] and trace gas concentration, including SO_2 [15], BrO [15], CH_2O [8,16], OClO [16], O_3 [17], CH_3COCOH [9], CHOOCH [9], I_2 [18], IO [18], OIO [18], NO_2 [19,20], HONO [18,20], OBrO and NO_3 [3–7,21]. Typical concentrations of these species in the troposphere are given in Table 1.

In this article, we overview our recent developments and applications of LED-IBBCEAS instruments [19–21] for: (1) simultaneous measurements of nitrous acid (HONO) and nitrogen dioxide (NO_2) in a field intercomparison campaign at a suburban site of Tung Chung in Hong Kong. The measurements by the IBBCEAS instrument showed good agreement with the data from commercial analytical instruments, while exhibiting the unique ability to perform direct concentration measurement (without any sample preparation and conversion) with high temporal resolution, compared to the commercially available chemical conversion-based instruments; (2) real-time optical tracking nitrate radical (NO_3) and NO_2 concentrations during a process of isoprene oxidation by NO_3 radical in a smog chamber. The measured NO_3 concentration-time profile allowed for direct determination (without reference) of this NO_3-initiated oxidation reaction rate constant via FACSIMILE chemical dynamics simulation.

#257569 Received 19 Jan 2016; revised 17 Feb 2016; accepted 19 Feb 2016; published 24 Mar 2016

Table 1. Typical tropospheric concentrations of some major gaseous molecules spectroscopically detectable in the UV-visible spectral region.

Species	Concentration	References
O_3	10 - 500 ppbv	[22]
SO_2	0.01 - 20 ppbv	[22,23]
NO_2	1 - 200 ppbv	[23]
CH_2O	0.1 - 60 ppbv	[22,23]
I_2	10 - 100 pptv	[24]
IO	up to 7 pptv	[24]
OIO	up to 10.8 pptv	[24]
OClO	up to 70 pptv	[25]
OBrO	up to 15 pptv	[25]
NO_3	1 - 200 pptv	[23,26]
HONO	0.1 - 10 ppbv	[20,23]
CHOCHO	up to 250 pptv	[9]
CH_3COCHO	up to 5.7 ppbv	[9]

2. Principle of IBBCEAS

The basic idea of the IBBCEAS technique is to couple incoherent broadband radiation into an optically stable high-finesse cavity, consisting usually of two mirrors with an averaged reflectivity $R(\lambda) = [R_1(\lambda)R_2(\lambda)]^{1/2}$, where $R_1(\lambda)$ and $R_2(\lambda)$ are respectively the reflectivities of mirror 1 and mirror 2, separated by a distance L. The transmission spectra of the cavity are measured first in the absence of absorbing species $I_0(\lambda)$ by purging the cavity with pure N_2 or zero air, and then in the presence of air sample $I(\lambda)$. Not only the absorptions by molecular species, but also Rayleigh scattering $\alpha_{Ray}(\lambda)$ by gaseous molecules and Mie scattering $\alpha_{Mie}(\lambda)$ by aerosol particle contribute to optical extinction inside the cavity. By taking into account of these scattering induced extinctions effects, the total optical extinction $\alpha(\lambda)$ can be described as [19]:

$$\alpha(\lambda) = \left(\frac{1 - R(\lambda)}{d} + \alpha_{Ray}(\lambda) + \alpha_{Mie}(\lambda) \right) \times \left(\frac{I_0(\lambda)}{I(\lambda)} - 1 \right) \quad (1)$$

where d is the interaction length of light with target species inside the cavity ($d \le L$).

As indicated in Eq. (1) above, for absolute concentrations retrieval, the wavelength-dependent mirror reflectivity $R(\lambda)$ must be known. In the case of using closed cavities, the mirror reflectivities can be measured using a broadband absorber with known concentration, such as NO_2 [3,21], O_2-O_2 [19], or using Rayleigh scattering spectra of two different scatterers, such as He / Zero air (N_2) [9] or CO_2 / N_2 [15]. $R(\lambda)$ can be also measured with phase-shift CRDS [7]. In open cavity configuration, Wu et al. [19] inserted a mobile PTFE tube between the cavity mirror mounts for mirror reflectivity calibration and spectral background measurement, and removed it out for open-path measurement. In open-path experiment, the absolute $R(\lambda)$ can be determined in two steps: at first, the shape of the wavelength-dependent relative $R(\lambda)$ is obtained from broadband absorption spectrum of NO_2 samples diluted in pure N_2 (with unknown concentration). This relative $R(\lambda)$ is then scaled to an absolute mirror reflectivity value determined with absorption of pure oxygen collisional pair O_2–O_2 (with known concentration).

Given the measured mirror reflectivity $R(\lambda)$ and the interaction length d, the target gas concentrations can be retrieved using least-squares fit [4,19] to the experimentally measured optical extinction $\alpha(\lambda)$:

$$\alpha(\lambda) = \sum_i n_i \cdot \sigma_i(\lambda) + a\lambda^2 + b\lambda + c \quad (2)$$

where $\sigma_i(\lambda)$ standards for the reference cross section ($cm^2.molecule^{-1}$) of i^{th} species and the reference cross sections should be convoluted with the measurement instrument function (i.e.

#257569 Received 19 Jan 2016; revised 17 Feb 2016; accepted 19 Feb 2016; published 24 Mar 2016

the resolution of the spectrometer). n_i is the concentrations (number densities in [molecule/cm^3]) of the i^{th} species. The second-order polynomial term in Eq. (2) represents background baseline, which could arise from gas scattering, LED intensity fluctuations, and other unspecified loss processes. The unknown parameters (number densities n_i, a, b and c) can be extracted using a linear algebraic method known as the singular value decomposition (SVD) method [4] that is more faster for real-time concentration retrieval than a nonlinear Levenberg–Marquardt routine [21].

3. Experimental apparatus and operation

3.1 Experimental set-up

Typical LED-IBBCEAS setups are schematically depicted in Fig. 2, including closed-cavity [20] and open-cavity configurations [19]. Open-path measurement is highly desired, which allows one to avoid cavity wall losses and sampling induced artifacts. However, for application in urban and coastal environments at heavy aerosol particles levels (where the extinction loss α_{Mie} is similar to, even higher than the mirror loss $(1-R(\lambda)/d)$), Mie scattering by aerosols might strongly shorten the wavelength-dependent effective cavity path length, and hence degrade the measurement sensitivity.

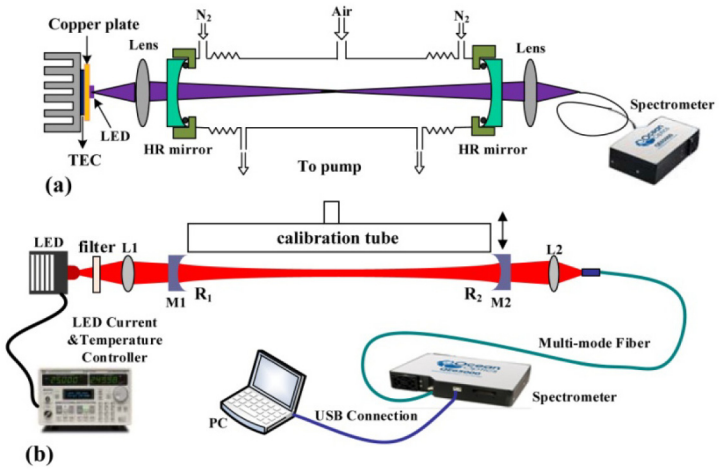

Fig. 2. Schematic diagrams of typical LED-IBBCEAS apparatus: (a) closed-cavity configuration [20]; (b) open-cavity scheme [19];

The LED source is mounted on a temperature controlled heat sink made of copper plate to stabilize the optical output intensity and spectral profile of the LED emission. The temperature is stabilized within ± 0.01 °C by means of a single-stage thermo electric cooler (TEC, PE-063-08-15, Supercool) associated with a temperature sensor (PT100, RTD or Analog device, AD590). A laser diode controller (LDC501, Stanford Research System) is used to supply electric power for both the TEC and the LED.

High optical-finesse cavity is formed with two high-reflectivity mirrors (Layertec GmbH), separated by a distance of $L \sim$ 1-2 m. Light from the LED is focused with a lens of f = 75 mm into the center of the optical cavity. The light transmitted through the cavity was collected into a multimode optical fiber (1000 μm in diameter) with a second f = 75 mm lens and then coupled to a CCD spectrometer (QE65000, Ocean optics). In order to avoid saturation of the CCD detector at the edges of high reflectivity range of the cavity mirrors, a band-pass filter is placed between the LED and the cavity to block the light at undesirable wavelength. A spectral resolution of <1 nm is necessary for selective recognition of the structured broadband absorption of target species (HONO, NO_3, NO_2) in the UV and visible region.

#257569 Received 19 Jan 2016; revised 17 Feb 2016; accepted 19 Feb 2016; published 24 Mar 2016

Figure 3(a-c) shows the LED-IBBCEAS instruments developed and deployed in our recent work for applications of high-sensitivity measurements of HONO, NO_3 and NO_2 in intensive field campaigns and in atmospheric simulation chamber.

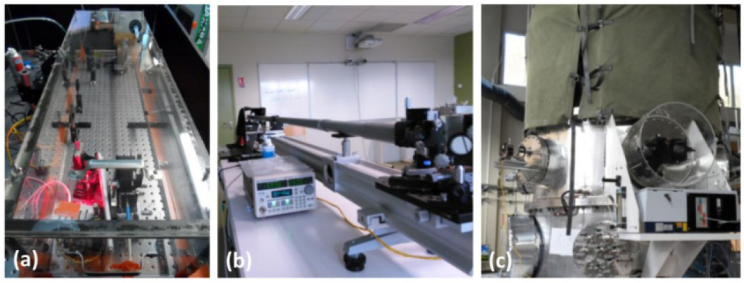

Fig. 3. Photographs of the recently developed IBBCEAS instruments for: (a) monitoring of ambient NO_3; (b) open-path detection of indoor HONO (a PVC tube is used for calibration of cavity mirror reflectivity and for measurements of background spectra $I_0(\lambda)$; (c) real-time tracking of HONO concentration in a chemical simulation chamber.

3.2 Detection limit and measurement precision

Figure 4 shows typical broadband (635-675 nm) absorption spectra of 324 pptv NO_3 and 735 ppbv NO_2 associated with the correspoding fits for their concentration retrieval. Open-cavity configuration (Fig. 2(b)) was involved in this IBBCEAS experiment dedicated to chemical kinetic study in a smog chamber (see Section 4.2. for details).

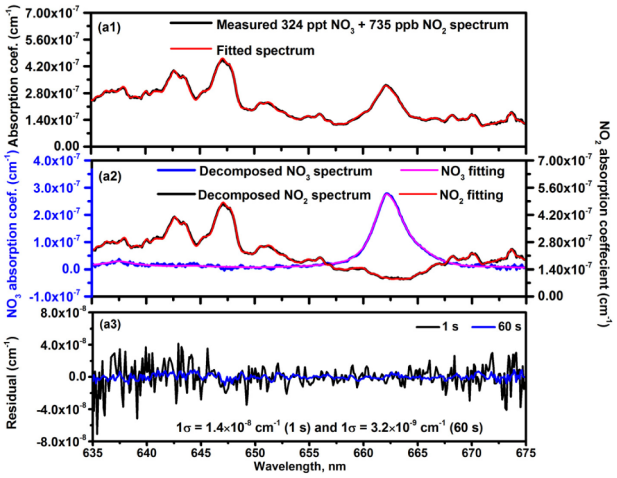

Fig. 4. (a1) Measured and fitted IBBCEAS spectra of 324 pptv NO_3 and 735 ppbv NO_2; (a2) Decomposed spectra and the related fits. (a3) Fit residual using 1 s and 60 s intergration time, respectively.

Minimum detectable concentrations (MDCs) of 16 pptv for NO_3 and 18 ppbv for NO_2 in 1 s integration time were deduced based on the fit residual shown in Fig. 4(a3). In the case of white noise limited measurement, these MDCs can be further improved down to 3.6 pptv for NO_3 and 4.1 ppbv for NO_2 by data averaging in 60 s.

The optimal integration (averaging) time can be obtained by an Allan variance analysis using usually time series IBBCEAS spectra of zero air (or N_2), recorded with a rate of 1 s per spectrum. Typical Allan variance analysis results (expressed in Allan deviation) are shown in Fig. 5, illustrating a maximum instrument stabilization time of ~100 s, which result in a measurement precision of ~1.7 pptv for NO_3 and ~1.6 ppbv for NO_2, respectively.

#257569 Received 19 Jan 2016; revised 17 Feb 2016; accepted 19 Feb 2016; published 24 Mar 2016

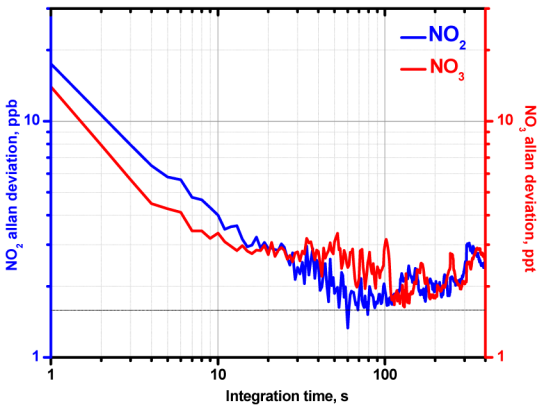

Fig. 5. Allan deviation plots showing a instrument stabilization time of ~100 s.

4. Applications

4.1 Optical monitoring of HONO and NO_2 in Hong Kong

HONO is a very important source of OH radicals. However the sources and sinks of HONO as well as their formation mechanism in the atmosphere are still not completely defined and understood. This is due to the difficulty in measuring this highly reactive short-lived species, though various instruments have been developed and field established [1].

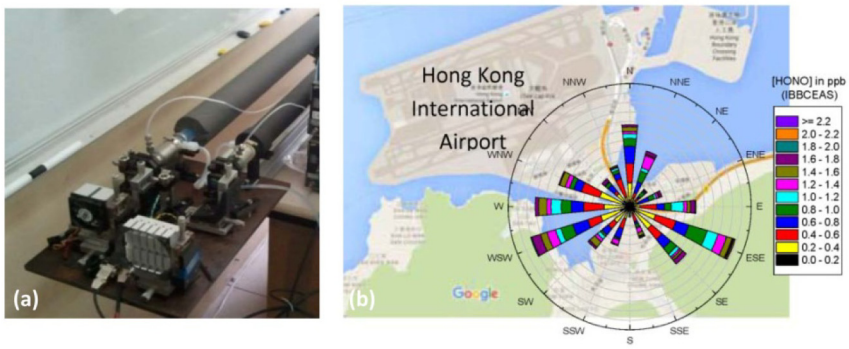

Fig. 6. (a) The LED-IBBCEAS setup used in Hong Kong compaign; (b) Wind rose plot showing the dependence of HONO concentration on the wind direction during the period of 7:10 on May 13rd to 10:50 on May 14th, 2012;

A UV LED-IBBCEAS instrument has been developped, as schematically depicted in Fig. 2(a), in this context for simultenous measurements of HONO and NO_2 in the environment. The used LED (Nichia, NCSU033AT) emitted ~250 mW optical power in the UV spectral region around 365 nm with a full width at half maximum (FWHM) of ~10 nm. The optical cavity (d = 1.76 m) was formed with two high reflectivity (~99.95% at 355 nm) mirrors having a radius of curvature of 2 m (Layertec GmbH), which resulted in a maximum effective path length of 3.52 km. The cavity mirrors housed in mirror mounts were purged with a constant flow of dry N_2 at a rate of 200 SCCM (Standard Cubic Centimeter Per Minute) to prevent the contamination of the cavity mirror by aerosols. The IBBCEAS spectra were recorded with a temperature stabilized UV CCD spectrometer (QE65000, Ocean optics) with a spectral resolution of ~0.53 nm. All of the optical components, including the UV LED, the optical cavity, the focusing lens and the fiber coupler were mounted on a 2 m long optical rail (Fig. 6(a)). An 2 μm pore size poly tetrafluoroethylene (PTFE) filter was used at the air inlet of the cavity to block aerosols entering the cavity. An oil-free diagram pump was used to pull

#257569 Received 19 Jan 2016; revised 17 Feb 2016; accepted 19 Feb 2016; published 24 Mar 2016

air through the optical cavity at a constant flow rate of 2 SLPM (Standard Liters Per Minute). 1σ (signal-to-noise ratio = 1) detection limits of 300 pptv for HONO and 1 ppbv for NO_2 were achieved using an optimum acquisition time of 120 s.

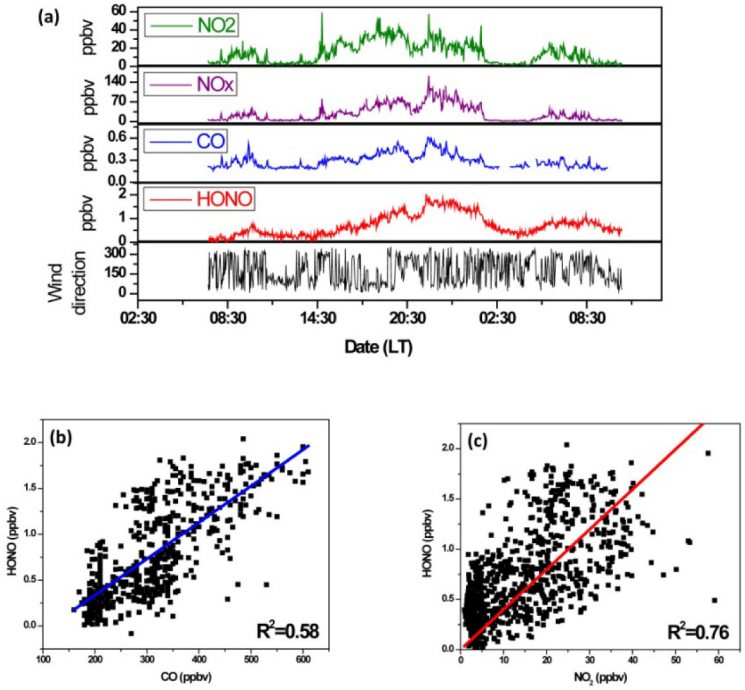

Fig. 7. (a) Time series measurements of wind direction and concentrations of NO_2, NOx, CO and HONO; (b) and (c) Correlation of HONO vs. CO and vs. NO_2, respectively.

This UV LED-IBBCEAS apparatus was deployed at a suburban site of Tung Chung (22.30° N, 113.93° E) in Hong Kong for simultaneous measurements of HONO and NO_2 in ambient air during a field intercomparison campaign [20]. Daytime and nighttime concentrations of HONO and NO_2 were recorded and compared, in good agreement, with data from a long path absorption photometer (LOPAP, QUMA, Model LOPAP-03) and from a NOx analyzer equipped with a blue light converter (TEI, Model 42CY), respectively.

Figure 7(a) shows time series measurements of HONO, NOx, CO and wind direction during the period between 7:10 on May 13rd and 10:50 on May 14th, 2012. High temporal correlations of HONO with CO (Fig. 7 (b)) and with NO_2 (Fig. 7(c)) were observed, which might allow for identification of HONO source that may be originated from local direct anthropogenic emissions resulting from combustion processes. In fact, the campaign measurement site Tung Chung (TC) is located on north Lantau Island and about 3 km southest of Hong Kong International airport on Chek Lap Kok (Fig. 6(b)). TC is located within a residential area in a new town, adjacent to the highway and to railway lines that connect the airport to the other islands of Hong Kong.

The HONO concentrations in relation to wind sector during this period is presented in Fig. 6(b). The wind rose plot shows that most of high HONO levels (up to ~2 ppbv) was associated with the wind coming from the airport and from the urban area involved in busy traffic activity.

The test of such a LED-IBBCEAS setup with the well established HONO and NO_2 measurement instruments, for the first time, in a real atmospheric environment, demonstrated the feasibility of the IBBCEAS technique for interference (chemical and spectral) free direct

#257569 Received 19 Jan 2016; revised 17 Feb 2016; accepted 19 Feb 2016; published 24 Mar 2016

concentration measurements of environmental HONO and NO_2, without any chemical conversion or sample preparation.

4.2 Optical traking of NO_3 and NO_2 in oxidation processes of isoprene in smog chamber

Isoprene (C_5H_8) is the most abundant non-methane hydrocarbon emitted from vegetation into the troposphere. Photochemical oxidation of isoprene has important implications for local and regional air quality, the greenhouse effect including ozone and acid production [27]. In the present work, we demonstrated for the first time direct determination of the rate constant of isoprene oxidation by NO_3 radicals using IBBCEAS measurement. The experiments were performed in a smog chamber operating at atmospheric pressure and room temperature (296 ± 2 K) under dry conditions (Relative Humidity: RH<1%). The smog chamber (Fig. 8, *left*) is made of an 8 m^3 plexiglas reactor [21]. A high power red LED (SMB660N-1100-01, Marubeni America Corp.) emitting around 660 nm with a 25 nm FWHM was used as probing light source. It emitted 300 mW optical power within a divergent angle of ± 7°. Two high reflectivity mirrors having a 6 m radius of curvature (Layertec GmbH) were installed on the smog chamber walls facing each other and separated by 2 m to form a high optical finesse cavity, as shown in Fig. 8 (*left*), based on the basic open-path IBBCEAS set-up presented in Fig. 2(b), without the calibration tube. In the present work, calibration of the cavity mirror reflectivity was carried out by injection of NO_2 (93 ppbv) into the smog chamber (the absolute NO_2 concentration was monitored by a chemiluminescence NOx analyzer, Model 42i, Thermo Inc.). Based on Eq. (1) and given the measured distance of $d = L = 2$ m between two cavity mirrors, the experimentally measured IBBCEAS absorption spectra of NO_2 with known concentration allowed us to determine the mirror reflectivity being between 99.96% and 99.97% (620-680 nm), leading to a maximum effective path length of ~6.7 km (at 662 nm). The used CCD spectrometer allows covering the spectral range of 570–732 nm with a spectral resolution of 0.42 nm. MDCs of 3.6 pptv for NO_3 and 4.1 ppbv for NO_2 were respectively achieved with an average time of 1 min. The chamber was initially purged with zero air (so as to render NO and NO_2 concentrations less than 1 ppbv), then background spectra $I_0(\lambda)$ were recorded. After that, about 2.0 ppm NO_2 were injected into the smog chamber, the NO_2 concetration was simultaneously measured with the red LED-IBBCEAS and a chemiluminescence NOx analyzer (Model 42i, Thermo Inc). Afterwards 1.6 ppm O_3 generated from an O_3 generator (Monitor Europe ML 9841B, Thermo Corp.) was introduced into the chamber to produce NO_3 via the reaction: $NO_2 + O_3 \rightarrow NO_3 + O_2$. Time series measurements of NO_2 and NO_3 concentrations were simultaneously performed using the red LED-IBBCEAS.

Based on Eqs. (1) and (2), considering the uncertainties in the cross section, in the cavity length, in the factor of $(1-R)$ and the uncertainty associated with the spectral fitting procedure, the total measurement uncertainties were approximately estimated to be 9.1% for NO_2 and 7.8% for NO_3 respectively. Indeed, NO_3 is very reactive and the NO_3 lifetime inside the smog chamber is about 67 s due to the chamber wall losses, determined in our previous work [21]. In this work, the NO_3 data acquisition time was 1 s, much less than its wall loss-limited lifetime, the measurement accuracy was thus mainly limited by the uncertainty in the available absorption cross sections used for the concentration retrieval.

Once the NO_3 concentration reached the maximum value of ~10 ppbv, about 40 ppbv C_5H_8 was introduced into the chamber. Oxidation of C_5H_8 by NO_3 radicals was tracked by real-time concentration measurements of NO_3 and NO_2 by the red LED-IBBCEAS, and isoprene concentration-time profile was measured with a proton transfer reaction mass spectrometry (PTR-MS, Ionicon Analytik GmbH). The rate constant for the NO_3 oxidation of isoprene was determined by fitting (Fig. 8, *right*) the measured concentration-time profiles of NO_3 and isoprene to a FACSIMILE simulation model [28].

#257569 Received 19 Jan 2016; revised 17 Feb 2016; accepted 19 Feb 2016; published 24 Mar 2016

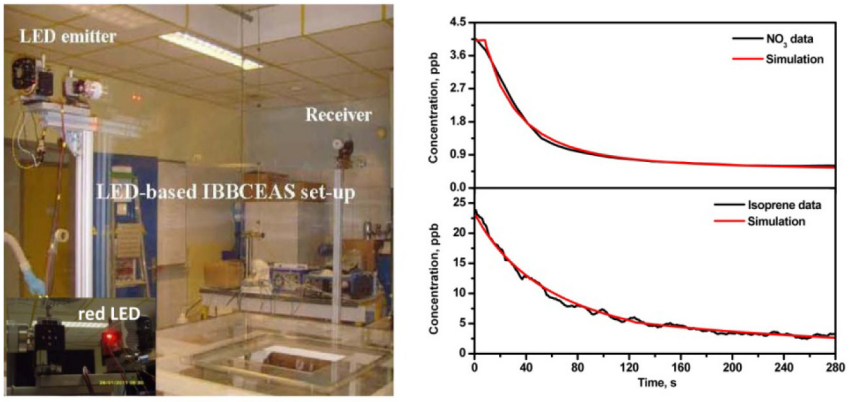

Fig. 8. *left*: The smog chamber equipped with an IBBCEAS apparatus for real-time traking chemical oxidation process. *right*: Fit of the FACSIMILE simulation model (red curves) to the measured concentration-time profiles (black) of NO_3 and C_5H_8 for direct determination of the reaction rate constant for the oxidation of C_5H_8 by NO_3.

Chemical reaction rate constant of $k_{isoprene} = (7.1 \pm 0.3) \times 10^{-13}$ $cm^3.molecule^{-1}.s^{-1}$ was deduced at 296 ± 2 K from the FACSIMILE simulation fit, and it is in good agreement with the most recommended value of $(6.9 \pm 0.2) \times 10^{-13}$ $cm^3.molecule^{-1}.s^{-1}$ [29,30], determined using relative rate method which needs a reference chemical reaction with known rate constant [29]. The present work demonstrated the high potential of IBBCEAS technique for direct and absolute rate constant determination without any references.

4. Conclusion

LED-IBBCEAS technique provides a high-sensitivity analytical tool for simultaneous monitoring of multi-species of atmospheric interest for field campaign application and smog chamber simulation study. This self-calibrated spectroscopic instrument also shows its interesting potential for use in validation and calibration of routinely used chemical analytical instruments.

Acknowledgments

The authors acknowledge financial supports from the French Agence Nationale de la Recherche (ANR) under the CaPPA (ANR-10-LABX-005) contract, the National Natural Science Foundation of China (NSFC: No.21307136) and (NSFC: No.41265011), as well as the support in the framework of the CPER CLIMIBIO program funded by Nord-Pas de Calais Region and the Ministère de l'Enseignement Supérieur et de la Recherche.

#257569 Received 19 Jan 2016; revised 17 Feb 2016; accepted 19 Feb 2016; published 24 Mar 2016